

KEK Preprint 96-177  
March 1997  
H

A Measurement of the Photon Structure Function  $F_2^\gamma$   
at  $Q^2 = 6.8 \text{ GeV}^2$

The AMY Collaboration



**National Laboratory for High Energy Physics, 1997**

KEK Reports are available from:

Technical Information & Library  
National Laboratory for High Energy Physics  
1-1 Oho, Tsukuba-shi  
Ibaraki-ken, 305  
JAPAN

Phone: 0298-64-5136  
Telex: 3652-534 (Domestic)  
(0)3652-534 (International)  
Fax: 0298-64-4604  
Cable: KEK OHO  
E-mail: Library@kekvax.kek.jp  
Internet: <http://www.kek.jp>

# A Measurement of the Photon Structure Function $F_2^\gamma$ at $Q^2 = 6.8 \text{ GeV}^2$

The AMY Collaboration

T. Kojima <sup>a,q</sup>, T. Nozaki <sup>b</sup>, K. Abe <sup>b</sup>, Y. Fujii <sup>b</sup>, Y. Kurihara <sup>b</sup>, M.H. Lee <sup>b</sup>,  
A. Maki <sup>b</sup>, T. Omori <sup>b</sup>, H. Sagawa <sup>b</sup>, Y. Sakai <sup>b</sup>, T. Sasaki <sup>b</sup>, Y. Sugimoto <sup>b</sup>,  
Y. Takaiwa <sup>b</sup>, S. Terada <sup>b</sup>, P. Kirk <sup>c</sup>, T.J. Wang <sup>d</sup>, A. Abashian <sup>e</sup>,  
K. Gotow <sup>e</sup>, L. Piilonen <sup>e</sup>, S.K. Choi <sup>f</sup>, C. Rosenfeld <sup>g</sup>, L.Y. Zheng <sup>g</sup>,  
R.E. Breedon <sup>h</sup>, Winston Ko <sup>h</sup>, R.L. Lander <sup>h</sup>, J. Rowe <sup>h</sup>, S.L. Olsen <sup>i</sup>,  
S.K. Sahu <sup>i,m</sup>, K. Miyano <sup>j</sup>, H. Miyata <sup>j</sup>, N. Nakajima <sup>j</sup>, M. Sato <sup>j</sup>,  
M. Shirai <sup>j</sup>, N. Takashimizu <sup>j</sup>, Y. Yamashita <sup>k</sup>, S. Schnetzer <sup>l</sup>, S. Behari <sup>m</sup>,  
S. Kobayashi <sup>m</sup>, A. Murakami <sup>m</sup>, J.S. Kang <sup>n</sup>, D.Y. Kim <sup>n</sup>, S.S. Myung <sup>n</sup>,  
H.S. Ahn <sup>o</sup>, S.K. Kim <sup>o</sup>, K. Ueno <sup>p</sup>, S. Matsumoto <sup>q</sup>, and T. Aso <sup>r</sup>,

<sup>a</sup> Toho High School, Tokyo 186, Japan

<sup>b</sup> KEK, National Laboratory for High Energy Physics, Ibaraki 305, Japan

<sup>c</sup> Louisiana State University, Baton Rouge, LA 70803, USA

<sup>d</sup> Institute of High Energy Physics, Beijing 100039, China

<sup>e</sup> Virginia Polytechnic Institute and State University, Blacksburg, VA 24061, USA

<sup>f</sup> Gyeongsang National University, Chinju 660-701, Republic of Korea

<sup>g</sup> University of South Carolina, Columbia, SC 29208, USA

<sup>h</sup> University of California, Davis, CA 95616, USA

<sup>i</sup> University of Hawaii, Honolulu, HI 96822, USA

<sup>j</sup> Niigata University, Niigata 950-21, Japan

<sup>k</sup> Nihon Dental College, Niigata 951, Japan

<sup>l</sup> Rutgers University, Piscataway, NJ 08854, USA

<sup>m</sup> Saga University, Saga 840, Japan

<sup>n</sup> Korea University, Seoul 136-701, Republic of Korea

<sup>o</sup> Seoul National University, Seoul 151-742, Republic of Korea

<sup>p</sup> National Taiwan University, Taipei 10764, China

<sup>q</sup> Chuo University, Tokyo 112, Japan

<sup>r</sup> Toyama National College of Maritime Technology, Toyama 933-02, Japan

**Abstract**

The photon structure function  $F_2^\gamma$  has been measured at an average  $Q^2$  value of  $6.8 \text{ GeV}^2$  using data collected by the AMY detector at the TRISTAN  $e^+e^-$  collider. The measured  $F_2^\gamma$  is compared with several QCD-based parton density models.

## 1 Introduction

Since the inclusive cross sections of deep-inelastic electron-photon scattering and high- $p_t$  jet production in two-photon collisions can be expressed in terms of the parton (quark and gluon) distribution functions of the photon [1, 2], the photon parton densities are, in principle, accessible from measurements of these processes. However, only the quark density, which can be determined from the photon structure function  $F_2^\gamma$  using deep-inelastic electron-photon scattering, is directly measurable. Thus, in practice, the measured values of  $F_2^\gamma$  are used to evaluate the predictions of various QCD-motivated models for the photon's quark and gluon density functions.

There are a number of models that give predictions for the photon parton density. In these models, the photon's parton density is calculated by solving the inhomogeneous Altarelli-Parisi (IAP) equations [3], where the low  $Q^2$  boundary condition at  $Q^2 = Q_0^2$  is fixed either by fitting the evolved  $F_2^\gamma$  to its measured values (type-1) [4, 5, 6] or by invoking model assumptions (type-2) [7, 8, 9]. In the very recent model (called SaS), the shapes of the input distributions are determined by the  $F_2^\gamma$  data, while the normalizations are constrained (type-3) [10]. Since the precision of existing  $F_2^\gamma$  determinations is still limited, additional measurements can help improve the parton density determinations of the type-1 and 3 models.

High energy  $e^+e^-$  collisions are well suited for the study of collisions of quasi-

real and virtual photons. Bremsstrahlung photons emitted from the beam particles have a considerable chance of colliding with each other and producing hadrons. We use the variables  $q$  and  $k$  to represent the four-momenta of the two photons that collide to produce the hadronic system. In the special case when  $k^2 \approx 0$  and  $-q^2 \gg 0$ , the electron associated with the  $q$ -photon gets scattered at a large angle, and is tagged in the detector, while the electron associated with the  $k$ -photon is scattered at a small angle close to the beam-line and escapes detection. Such a process can be described as the deep-inelastic electron-photon scattering, with the target photon being the  $k$ -photon.

In terms of laboratory variables, the cross section for this process is given by [11, 1]

$$\frac{d\sigma}{dE_{tag} d \cos \theta_{tag}} = \frac{4\pi\alpha^2 E_{tag}}{Q^4 y} \left[ \left\{ 1 + (1-y)^2 \right\} F_2^\gamma(x, Q^2) - y^2 F_L^\gamma(x, Q^2) \right], \quad (1)$$

where  $Q^2 = -q^2 = 4E_{tag}E_{beam} \sin^2(\theta_{tag}/2)$ , and  $\theta_{tag}$  and  $E_{tag}$  are the scattering angle and energy of the tagged electron. The scaled variable  $x = \frac{Q^2}{Q^2 + W^2}$  represents the momentum fraction carried by the struck parton inside the photon, and  $y = 1 - \frac{E_{tag}}{E_{beam}} \cos^2(\theta_{tag}/2)$ . Here  $W$  is the invariant mass of the produced hadronic system.

The contribution from the  $F_L^\gamma$  structure function in Eq.(1) is estimated to be negligibly small compared to the total for the kinematical conditions of the present experiment. Thus, measurements of the cross section of Eq.(1) provide a rather direct determination of  $F_2^\gamma$ .

We present here measurements of the photon structure function  $F_2^\gamma$  at an average  $Q^2$  value of 6.8 GeV<sup>2</sup>. Measurements of  $F_2^\gamma$  for higher  $Q^2$  values using the AMY data are reported in ref. [12, 13]. We compare our results with those from the other experimental groups [14, 15, 16, 17] at similar  $Q^2$  values. The results are

also compared with several parameterizations of the parton density in the photon.

## 2 Experimental Apparatus and Event Selection

The data used are obtained with the upgraded AMY detector (called AMY 1.5) at the TRISTAN  $e^+e^-$  collider at  $\sqrt{s} = 58$  GeV and corresponds to an integrated luminosity of 239.6 pb<sup>-1</sup>. A detailed description of the AMY 1.5 detector is given in ref. [18]. We briefly note here features of the detector that are important for this analysis.

Charged particles are detected in a cylindrical drift chamber (CDC) with an acceptance of  $|\cos \theta| < 0.906$  and momentum resolution  $\Delta p_t/p_t^2 \simeq 0.6\%$  GeV<sup>-1</sup>. A cylindrical, lead/proportional-tube barrel electromagnetic shower counter (SHC) surrounds the CDC and has an acceptance of  $|\cos \theta| < 0.75$ . A lead/scintillator endcap shower counter (ESC) covers the region  $10.8^\circ < \theta < 37^\circ$  in both the forward and backward directions. A small angle shower counter (SAC), situated inside the ESC, consists of arrays of defining scintillation counters, silicon-pad position detectors and a lead-scintillator calorimeter. It extends the angular coverage down to  $\theta = 3^\circ$  with an energy resolution of  $\Delta E/E = \sqrt{(17.9/\sqrt{E} - 0.34)^2 + (10.4/E)^2}\%$  where  $E$  is in GeV and angular resolutions of  $\sigma(\theta) = 0.16^\circ$  and of  $\sigma(\phi) = 0.67^\circ$ . The SAC is used to tag the scattered electrons that are the subject of this analysis.

Candidate tagged events are selected using the following criteria :

1. A candidate tagged electron is identified with an SAC energy cluster that is in the  $4^\circ < \theta < 7^\circ$  angular region with energy above [31.61 - 1.66  $\theta$  (in degrees)] GeV and below 28 GeV.
2. No additional clusters with energy greater than  $0.25E_{beam}$  are observed else-

where in the detector and the total energy observed in the ESC and SAC on the opposite side from the tagged electron is less than  $0.25E_{beam}$  (anti-tagging cut).

3. At least three charged particles are seen in the CDC, at least two of which have  $p_T \geq 750$  MeV.
4. A total visible energy of the detected charged and neutral particles,  $E_{vis}$ , that is less than  $0.25E_{beam}$ .
5. An observed invariant mass of the produced hadronic system,  $W_{vis}$ , that is greater than 1 GeV.
6. A Normalized Longitudinal Momentum Imbalance,  $NLMB$ , that is greater than 0.3, where  $NLMB = \Sigma p_L / E_{beam}$  along the tag direction, with the sum running over all charged and neutral particles, including the tagged electron.

The 28 GeV maximum energy cut for tagged electrons is imposed to exclude contamination of Coulomb-scattered beam gas events in accidental coincidence with untagged two-photon events. The angle-dependent minimum energy cut for tag electrons is required to remove contamination from off-energy beam particles that are overfocused by the interaction region quadrupole magnets into the SAC. All the physical quantities such as  $E_{vis}$ ,  $W_{vis}$  etc. are calculated excluding clusters observed in the SAC because of the high rate of beam-related background tracks in these devices.

A total of 770 events pass these cuts. We calculate backgrounds using Monte Carlo simulations. The background level from  $e^+e^- \rightarrow e^+e^-\tau^+\tau^-$  is  $29.8 \pm 1.1$  events, which includes a trigger efficiency correction. Backgrounds from inelastic Compton scattering [19], multihadronic annihilation events and  $e^+e^- \rightarrow \tau^+\tau^-$  are negligibly small.

After the background subtraction,  $740 \pm 28$  events remain. The trigger efficiency was determined from redundant, independent triggers to be  $78.0 \pm 4.4\%$ . The  $Q^2$  values for these events range from 3.5 to 12 GeV<sup>2</sup>, with an average value of 6.8 GeV<sup>2</sup>.

### 3 Event Simulation

In order to make acceptance corrections for the unfolding procedure and to decide on kinematic cuts, we generated a large sample of Monte Carlo events that simulate the  $e^+e^- \rightarrow e^+e^- + hadrons$  process. The details of the Monte Carlo simulation are described in ref. [13] and are only briefly discussed here.

Monte Carlo events are generated according to the Field, Kapusta and Poggioli (FKP) [20], quark-parton (QPM) [21] and vector-meson dominance (VMD) [22] models. Contributions from the point-like part of  $F_2^\gamma$  to light-quark (i.e.  $u, d, s$ ) production are simulated by means of the FKP formalism [20, 12] using  $\Lambda = 0.2$  GeV for the QCD scale parameter and  $p_t^0 = 0.5$  GeV as the cut-off defining the boundary between the point-like and hadron-like regimes of the photon. The  $c$ -quark contribution to the point-like part of  $F_2^\gamma$  is generated using QPM [21]. For the hadronic part of  $F_2^\gamma$  we used the TPC/2 $\gamma$  group's parameterization of the VMD model [15] with a transverse momentum distribution that has the form  $\frac{d\sigma}{dp_T^2} \propto e^{-\beta p_T^2}$ , where  $p_T$  represents the transverse momentum of the quark with respect to the incident photon direction. We use  $\beta=3$ ,  $m_u = m_d = 325$  MeV,  $m_s = 500$  MeV and  $m_c = 1.6$  GeV. As mentioned above, contributions from the longitudinal structure function  $F_L^\gamma$  are neglected. The generated events are passed through the AMY detector simulation program and analysed with the same programs that are used for the real data.

There are two implicit assumptions in the MC simulation. The first is that the

target photon mass is zero. The second is that initial-state radiative corrections are negligibly small. In order to estimate these effects, we compared a QPM event sample generated for the heavy quark using our Monte Carlo with a sample produced by a generator developed by Berends, Daverveldt and Kleiss [23]. The latter is based on the exact calculation for all first order diagrams including radiative corrections. The quark mass dependence of the radiative corrections is assumed to be much smaller than the effects themselves and neglected. The resulting ratio of the cross sections of the BDK Monte Carlo and our Monte Carlo is 1.022, and this factor is used to correct our Monte Carlo yield.

After applying the experimental cuts, the relative contributions from the different MC event types are found to be in the ratio of

$$FKP : QPM : VMD = 51 : 20 : 29.$$

The expected number of events determined from the Monte Carlo calculations is  $769 \pm 6.4$ , which agrees well with the  $740 \pm 28$  events in the data sample. We see good agreement between the data and MC event samples for various kinematic variable distributions, such as  $NLMB$ ,  $W_{vis}$ ,  $E_{vis}$ , number of charged/neutral tracks,  $Q^2$ , and the polar angle and energy of the tagged electron.

The authors of the SaS model criticize the FKP+VMD model on three counts: 1) The hadronic part of  $F_2^\gamma$  given by  $TPC/2\gamma$  parameterization does not have a proper QCD  $Q^2$  evolution. 2) A strong correlation between the scale  $p_t^0$  and the size/shape of the hadronic part is neglected. 3) The FKP formula is a poor parameterization of the anomalous part. Therefore the FKP+VMD model is expected to provide only an approximate prediction of  $F_2^\gamma$ . However, we take the good agreement between the various distributions for the data and MC event samples as evidence that our Monte Carlo simulation provides an adequate estimate of the acceptance correction.

## 4 Analysis and Result

In order to extract  $F_2^\gamma$ , we correct the experimental data for detector acceptance effects by using the energy ratio method described in ref. [24]. In this method, fitted values of the four momentum of the photon-photon system and the energy of the tagged electron are determined by minimizing the  $\chi^2$  value of these quantities under the constraints of four momentum conservation. The fitted energy value of the photon-photon system,  $E^{cf}$ , is then used to calculate the estimated visible energy ratio  $\rho = E^{vis}/E^{cf}$ . The ratio of  $W_{vis}/W_{true}$  for MC events is plotted as a function of  $\rho$  and fit to a polynomial function. This fit is used to correct  $W_{vis}$ . Using the corrected  $W_{vis}$  we obtain the corrected  $x_{vis}$ , which we call  $x_{cor}$ .

The resulting data are then unfolded by using the unfolding technique described in ref. [25], which corrects for the effects of the detector resolution. We used  $x_{cor}$  and  $Q^2$  as the unfolding variables. The resulting  $F_2^\gamma$  values for different  $x$ -bins are presented in Table 1.

Table 1. Unfolded  $F_2^\gamma$  measurements.

$\langle Q^2 \rangle$	$x$	$\langle F_2^\gamma/\alpha \rangle$
6.8 GeV <sup>2</sup>	0.015-0.125	$0.337 \pm 0.030 \pm 0.044$
	0.125-0.375	$0.302 \pm 0.040 \pm 0.029$
	0.375-0.625	$0.322 \pm 0.049 \pm 0.084$

In Table 1, the first errors are statistical and the second are systematic. The systematic errors are the quadratic sum of the following:

- a 1.5% error due to the uncertainty in the measurement of luminosity;
- a 4.4% error due to the uncertainty in the trigger efficiency;

- an error ranging from 7.7 ~ 23 % due to the event selection cuts and background rejection;
- an error ranging from 1.6 ~ 11 % due to the uncertainty in the fragmentation function. This is determined from the variation of the unfolded  $F_2^\gamma$  determined using different fragmentation models : (a) LUND 6.2 fragmentation default parameters [26]; (b) LUND 6.2 tuned for TRISTAN data [27]; and (c) independent fragmentation model [28].

The measured  $F_2^\gamma$  function is shown in Fig. 1, where the error bars indicate the quadratic sum of the statistical and systematic uncertainties. Also shown in the figure are the experimental results of PLUTO[14], TPC/2 $\gamma$ [15], TOPAZ[16], and OPAL[17] at similar  $Q^2$  values.

In Fig. 2, we compare the measured  $F_2^\gamma$  function with the QCD-based theoretical prediction of the type-3, SaS model. This model has four sets of leading order (LO) parameterizations, SaS1D, SaS1M, SaS2D, and SaS2M. The first two sets are obtained by fixing normalization of the input distributions from the  $\gamma p$  analysis for the assumed  $Q_0$  value of 0.6 GeV and by fitting the shape of the input distributions to the  $F_2^\gamma$  data. The last two are obtained by using  $Q_0 = 2$  GeV and by fitting both the normalization and the shape of the input distributions to the  $F_2^\gamma$  data. The first and third sets are parameterizations in the DIS scheme, while the second and fourth sets are parameterizations in the  $\overline{MS}$  scheme. Since the DIS and  $\overline{MS}$  parameterizations provide similar  $F_2^\gamma$  functions for  $x$  values that are below 0.7, we chose to compare data with SaS1D and SaS2D only. As can be seen in the figure, the data are consistent with both predictions so that our data can not distinguish between the two predictions. Also shown in the figure is the Glück-Reya-Vogt (GRV), type-2 model prediction [7]. The GRV model provides both the LO and higher order (HO) predictions, but we only show the LO result

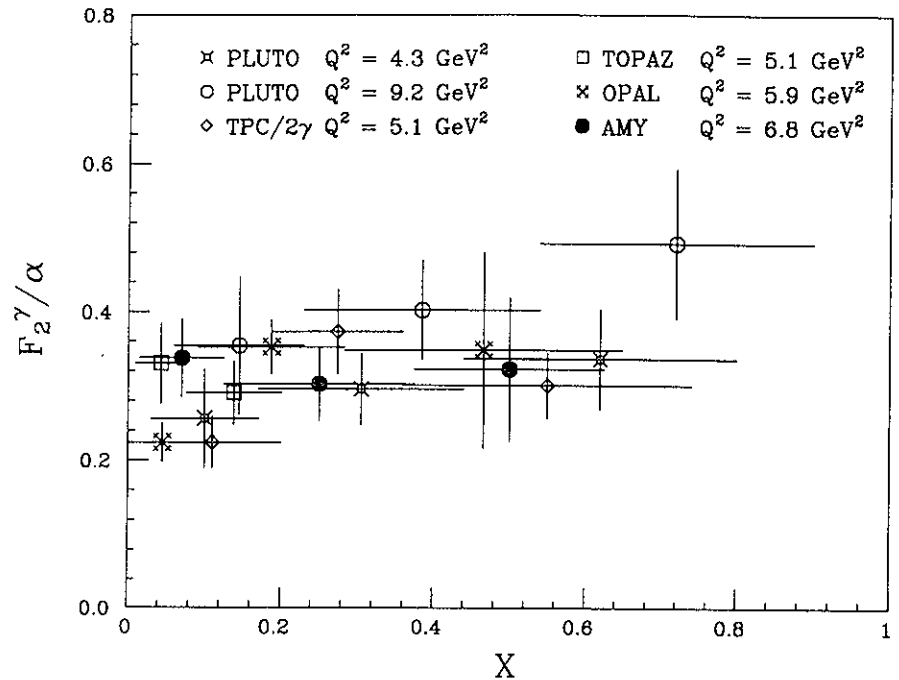


Figure 1: The measured  $F_2^\gamma$  values are compared with the other experimental results at the  $Q^2$  values around 7 GeV<sup>2</sup>.

since their difference are quite small in the kinematic region of this measurement. The GRV model fixes the input distributions from the ones of pions assuming  $Q_0^2$  (LO)= 0.25 GeV<sup>2</sup> and  $Q_0^2$  (HO)= 0.3 GeV<sup>2</sup>. The data are also consistent with the GRV prediction.

In Fig. 3 we compare the  $F_2^\gamma$  measurement with some predictions of the type-1 models, such as those of the Levy-Abramowicz-Charchula (LAC1) [5] model<sup>1</sup>, and the Watanabe-Hagiwara-Izubuchi-Tanaka (WHIT) [6] model.<sup>2</sup> The WHIT model predictions are in good agreement with the data. The LAC1 prediction agrees with the two higher  $x$  bin measurements, but disagree with the measurements in the lowest  $x$  bin. A similar behaviour at low  $x$  values can be seen in the TOPAZ measurements, shown in Fig. 1, and in  $Q^2 = 12$  GeV<sup>2</sup> DELPHI measurements [30] (not shown in Fig. 1). In contrast, the PLUTO, TPC/2 $\gamma$ , and OPAL results are consistent with the LAC1 prediction. Our previously reported measurements at  $Q^2 = 73$  GeV<sup>2</sup> [13] do not access the  $x < 0.1$  region where the differences between LAC1 and other models are more significant and, therefore, cannot distinguish between them. Although the experimental results of the jet production cross section in the photon-photon reaction are consistent with LAC1, the contribution from the low- $x$  component of the quark cannot be distinguished from the contributions of the quark and gluon distributions in other  $x$  regions [29].

The WHIT prediction explicitly takes into account the heavy quark mass effects, but the other calculations neglect them. Thus, the  $F_2^\gamma$  predictions of the SaS, LAC and GRV models are taken to be the sum of the QCD prediction for the light quarks and the QPM prediction for the  $c$ -quark, while the WHIT model gives

<sup>1</sup>Of the three LAC models, LAC1 and LAC2 give similar  $F_2^\gamma$  functions and LAC3 has already been experimentally rejected[29]. We, therefore, only compare our results with LAC1.

<sup>2</sup>Of the six versions of the WHIT model, we only show the WHIT1, WHIT4 and WHIT6 result; the other models have similar  $F_2^\gamma$  functions, differing only at very low  $x$  values.

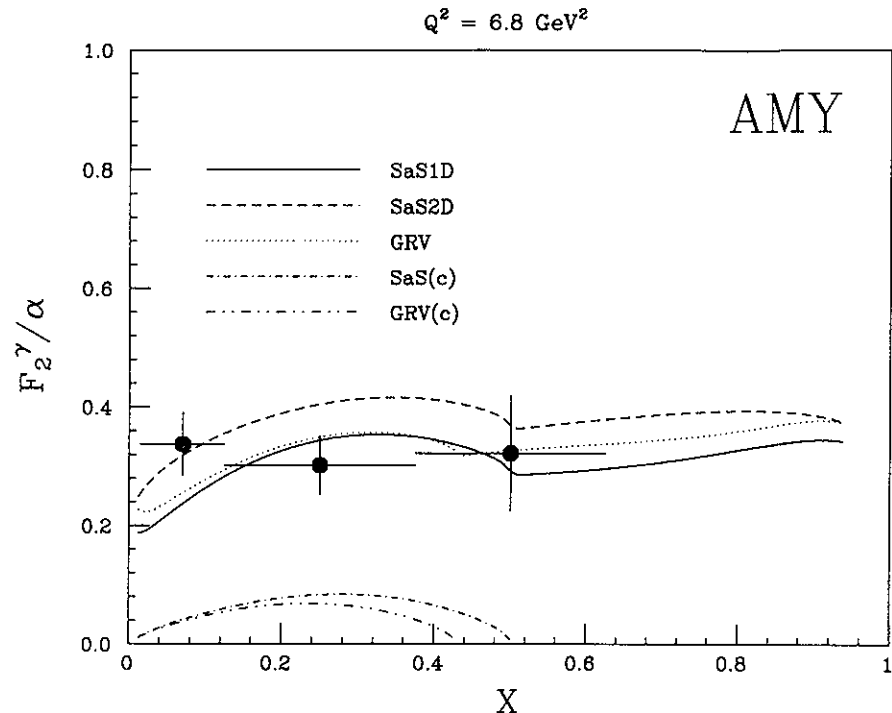


Figure 2: The  $F_2^\gamma$  values as a function of  $x$ . The data (closed circles) are compared with the SaS1D(solid), SaS2D (dashed) and GRV (dotted) model predictions. The heavy quark contributions for the SaS (dot-dashed) and the GRV (double-dot-dashed) models are shown separately.



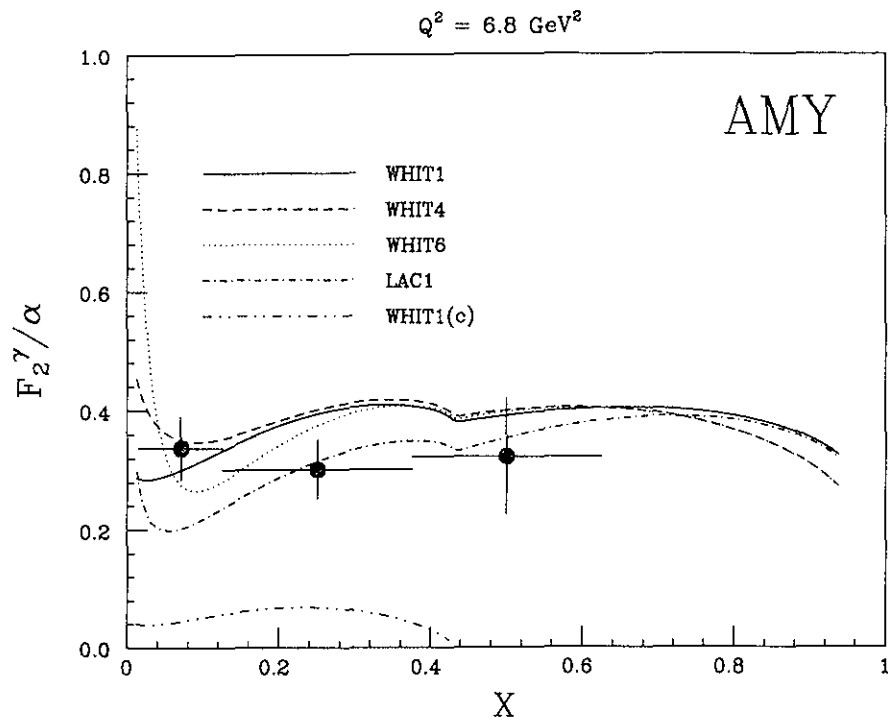


Figure 3: The  $F_2^\gamma$  values as a function of  $x$ . The data (closed circles) are compared with the WHIT1(solid), WHIT4 (dashed), WHIT6 (dotted) and LAC1 (dot-dashed) model predictions. The heavy quark contribution for the WHIT1 (double-dot-dashed) model is shown separately. The heavy quark contribution for LAC1 model, which is the same as for GRV, is shown in Fig. 2.

QCD predictions for  $F_2^\gamma$  for all flavors. Since the input parton distributions for the SaS, LAC and WHIT models are determined by fitting the evolved  $F_2^\gamma$  functions for the light quarks plus the  $c$ -quark contributions to the data, the  $F_2^\gamma$  predictions of these models for the light quarks depend on the assumed value of the  $c$ -quark mass. The LAC and WHIT models assume  $m_c = 1.5 \text{ GeV}$ , while SaS assumes  $m_c = 1.3 \text{ GeV}$ . We take  $m_c = 1.5 \text{ GeV}$  for GRV as suggested by the authors of GRV.

## 5 Summary

In summary, we have measured the photon structure function  $F_2^\gamma$  at  $Q^2 = 6.8 \text{ GeV}^2$ . The  $x$  behaviour of the measured  $F_2^\gamma$  are consistent with the QCD-based predictions such as SaS, GRV and WHIT models, but inconsistent with the LAC1 prediction for  $x$  values around 0.07

## 6 Acknowledgement

We thank the TRISTAN staff for the excellent operation of the storage ring. We acknowledge the strong support provided by the staffs of our home institutions. This work has been supported by the Japan Ministry of Education, Science and Culture (Monbusho), the Japan Society for the Promotion of Science, the US Department of Energy, the US National Science Foundation, the Korean Science and Engineering Foundation, the Ministry of Education of Korea, and the Academia Sinica of the People's Republic of China.

## References

- [1] Ch. Berger and W. Wagner, Phys. Rep. **146** (1987) 1.

- [2] M. Drees and R. Godbole, J. Phys. **G21** (1995) 1559.
- [3] M. Glück and E. Reya, Phys. Rev. **D28** (1983) 2749; M. Glück, K. Grassi, and E. Reya; Phys. Rev. **D30** (1984) 1447.
- [4] M. Drees and K. Grassie, Z. Phys. **C28** (1985) 451.
- [5] H. Abramowitz, K. Charchula and A. Levy, Phys. Lett. **B269** (1991) 458.
- [6] K. Hagiwara, M. Tanaka, I. Watanabe and T. Izubuchi, Phys. Rev. **D51** (1995) 3197.
- [7] M. Glück, E. Reya and A. Vogt, Phys. Rev. **D46** (1993) 1973.
- [8] P. Aurenche, J.-Ph. Guillet and M. Fontannaz, Z. Phys. **C64** (1994) 621.
- [9] L.E. Gordon and J.K. Storrow, Z. Phys. **C56** (1992) 307.
- [10] G.A. Schuler and T. Sjöstrand, Z. Phys. **C68** (1995) 607.
- [11] S.J. Brodsky, T. Kinoshita and H. Terazawa, Phys. Rev. Lett. **27** (1971) 280; Phys. Rev. **D4** (1971) 1532.
- [12] AMY Collab., T. Sasaki et al., Phys. Lett. **B252** (1990) 491.
- [13] AMY Collab., S.K. Sahu et al., Phys. Lett. **B346** (1995) 208.
- [14] PLUTO Collab., Ch. Berger et al., Phys. Lett. **B142** (1984) 111; Nucl. Phys. **B281** (1987) 365.
- [15] TPC/2 $\gamma$  Collab., H. Aihara et al., Z. Phys. **C34** (1987) 1.
- [16] TOPAZ Collab., K. Muramatsu et al., Phys. Lett. **B332** (1994) 478.
- [17] OPAL Collab., R. Akers et al., Z. Phys. **C61** (1994) 199.
- [18] AMY Collab., Y. Sugimoto et al. Phys. Lett. **B369** (1996) 86.
- [19] C. Peterson et al., Nucl. Phys. **B174** (1980) 424.
- [20] J.H. Field, F. Kapusta, and L. Poggioli, Phys. Lett. **B181** (1986) 362; Z. Phys. **C36** (1987) 121; F. Kapusta, Z. Phys. **C42** (1989) 225.
- [21] V.M. Budnev et al., Phys. Rep. **15** (1975) 181.
- [22] J.J. Sakurai and D. Schildknecht, Phys. Lett. **B40** (1972) 121.
- [23] F.A. Berends, P.H. Daverveldt and R. Kleiss, Comp. Phys. Comm. **40** (1986) 271; Nucl. Phys. **B253** (1985) 441.
- [24] J.S. Steinman, UCLA report, UCLA-HEP-88-004.
- [25] JADE Collab., W. Bartel et al., Z. Phys. **C24** (1984) 231.
- [26] T. Sjöstrand, Comp. Phys. Comm. **39** (1986) 347; T. Sjöstrand and M. Bengtsson, Comp. Phys. Comm. **43** (1987) 367.
- [27] AMY Collab., Y.K.Li et al., Phys. Rev. **D41** (1990) 2675.
- [28] R.D. Field and R.P.Feynman, Nucl. Phys. **B136** (1978) 1.
- [29] AMY Collab., B.J. Kim et al. Phys. Lett. **B325** (1994) 248.
- [30] DELPHI Collab., P. Abreu et al., Z. Phys. **C69** (1996) 223.